Comput. Methods Appl. Mech. Engrg. 199 (2010) 2987–2995

Contents lists available at ScienceDirect

Comput. Methods Appl. Mech. Engrg.

journal homepage: www.elsevier.com/locate/cma

A note on stochastic elliptic models

Xiaoliang Wan *

Department of Mathematics and Center for Computation and Technology, Louisiana State University, Baton Rouge, LA 70803, United States

ARTICLE INFO

Article history:
Received 24 November 2009
Received in revised form 12 May 2010
Accepted 8 June 2010
Available online 16 June 2010

Keywords:
Wiener chaos expansion
Wick product
Stochastic elliptic PDE
Uncertainty quantification

ABSTRACT

There exist two types of commonly studied stochastic elliptic models in literature: (I) $-\nabla\cdot(a(\boldsymbol{x},\omega)\nabla u(\boldsymbol{x},\omega))=f(\boldsymbol{x})$ and (II) $-\nabla\cdot(a(\boldsymbol{x},\omega)\diamondsuit\nabla u(\boldsymbol{x},\omega))=f(\boldsymbol{x})$, where ω indicates randomness, $\diamondsuit$ the Wick product, and $a(\boldsymbol{x},\omega)$ is a positive random process. Model (I) is widely used in engineering and physical applications while model (II) is usually studied from the mathematical point of view. The difference between the above two stochastic elliptic models has not been fully clarified. In this work, we discuss the difference between models (I) and (II) when $a(\boldsymbol{x},\omega)$ is a log-normal random process. We show that the difference between models (I) and (II) is mainly characterized by a scaling factor, which is an exponential function of the degree of perturbation of $a(\boldsymbol{x},\omega)$. We then construct a new stochastic elliptic model (III): $-\nabla\cdot((a^{-1})^{\diamondsuit(-1)}\diamondsuit\nabla u(\boldsymbol{x},\omega))=f(\boldsymbol{x})$, which has the same scaling factor as model (I). After removing the divergence from the scaling factor, models (I) and (III) can be highly comparable for many cases. We demonstrate this by a numerical study for a one-dimensional problem.

1. Introduction

Stochastic elliptic models are of fundamental importance for the stochastic modeling of physical and engineering applications [14,7]. For example, in reservoir and groundwater simulations, it is more appropriate to consider the permeability of porous media as a spatial random process instead of a deterministic function. Then, we need to construct a stochastic version of the Darcy's law. Based on different modeling strategies, the following two stochastic models

$$-\nabla\cdot(a(\boldsymbol{x},\omega)\nabla u(\boldsymbol{x}))=f(\boldsymbol{x}), \tag{1}$$

$$-\nabla\cdot(a(\boldsymbol{x},\omega)\diamondsuit\nabla u(\boldsymbol{x}))=f(\boldsymbol{x}) \tag{2}$$

have been widely studied in literature, where ω indicates randomness and $\diamondsuit$ the Wick product.

In Eq. (1), a random coefficients $a(\boldsymbol{x},\omega)$ is used to replace the effective coefficient $\hat{a}(\boldsymbol{x})$ in a deterministic model. Note here that the relation between $\mathbb{E}[a](\boldsymbol{x})$ and $\hat{a}(x)$ is usually model dependent. Eq. (1) usually implies that $\hat{a}(\boldsymbol{x})\neq\mathbb{E}[a](\boldsymbol{x})$ due to the closure for the moment equations; Eq. (2) corresponds to a deterministic elliptic equation with a coefficient $\hat{a}(\boldsymbol{x})=\mathbb{E}[a](\boldsymbol{x})$ for the mean solution due to the properties of the Wick product. If we want to apply the Lax–Milgram lemma to Eq. (1), a strong ellipticity condition is needed for the wellposedness, in other words, $a(\boldsymbol{x},\omega)$ must be strictly positive from below almost surely [1,5]. Such a strong ellipticity condition will directly affect the dimension reduction of $a(\boldsymbol{x},\omega)$. For example, one approach to approximate $a(\boldsymbol{x},\omega)$ is the Karhunen–Loève (K–L) expansion $a(\boldsymbol{x},\omega):=\mathbb{E}[a](\boldsymbol{x})+\sum_{i\geqslant 1}h_i(\boldsymbol{x})\xi_i$, where ξ_i are uncorrelated zero-mean random variables and $h_i(\boldsymbol{x})$ are deterministic functions defined by the correlation function of $a(\boldsymbol{x},\omega)$. To maintain the strong ellipticity, such a K–L expansion of $a(\boldsymbol{x},\omega)$ is usually modified to satisfy the following two extra conditions: (1) the number of ξ_i is finite, and (2) the support of ξ_i is compact. Then for a relatively low degree of perturbation, the strong ellipticity condition can be achieved. Another popular approach to define $a(\boldsymbol{x},\omega)$ is to consider a nonnegative function of a Gaussian random field, such as a log-normal [4] random field, where the probability of $a(\boldsymbol{x},\omega)$ approaching zero decays exponentially. The log-normal random field is widely used in engineering applications to model the physical properties of materials, such as the permeability in porous media. Although numerical computation shows that the solution of Eq. (1) for a log-normal coefficient $a(\boldsymbol{x},\omega)$ is square integrable in the probability space, the strong ellipticity still fails since a log-normal random field is not strictly positive from below, which implies that the Lax–Milgram lemma cannot be applied directly. Then we have to study the solution in a space larger than $L_2(\mathbb{F})$, where we usually associate a weight either to the probability measure or to each term of the orthonormal basis of the $L_2(\mathbb{F})$ space [7,12,9,13], see Section 3.2, where $\mathbb{F}$ indicates a complete probability space.

In Eq. (2), the regular product is replaced by the Wick product. The Wick product is a regularization procedure to alleviate the singularity induced by the noise. Mathematically speaking, it is a version of Malliavin divergence operator corresponding to the Itô-Skorohod integral. For example, the model

* Tel.: +1 225 578 6367.
E-mail address: xlwan@math.lsu.edu
URL: http://www.math.lsu.edu/~xlwan

0045-7825/$ - see front matter © 2010 Elsevier B.V. All rights reserved.
doi:10.1016/j.cma.2010.06.008

$$\dot{u}(t) = a(u(t)) + b(u(t)) \diamondsuit \dot{W}$$

is equivalent to the stochastic Itô differential equation

$$\dot{u}(t) = a(u(t)) + b(u(t)) dW_t,$$

where W_t indicates a standard Brownian motion and $\dot{W}$ white noise. Eq. (2) can be regarded as an extension of the Itô's stochastic integral to spatially-dependent noise. Although the singularity induced by noise is indeed alleviated by the Wick product to some extent [9], we, in general, still need the weighted $L_2(\mathbb{F})$ space to study the solution existence of Eq. (2), see Section 3.2, when $a(\boldsymbol{x},\omega)$ is log-normal. In contrast to Eq. (1), the solution of Eq. (2) is much more controllable through the weighted $L_2(\mathbb{F})$ space and a strong ellipticity condition is usually needed just for $\mathbb{E}[a](\boldsymbol{x})$ [9].

From the numerical point of view, the computation cost for approximating Eqs. (1) and (2) can be significantly different. In this work, we will employ a non-sampling technique, Winer chaos expansion, to deal with both Eqs. (1) and (2). For a log-normal coefficient $a(\boldsymbol{x},\omega)$, both solutions of Eqs. (1) and (2) have a unique Wiener chaos expansion. However, the cost to obtain the chaos coefficients for Eq. (1) is in general quadratic because the partial differential equations (PDEs) for the chaos coefficients are coupled together; however, the cost for Eq. (2) is linear due to the lower-triangular structure of the PDE system induced by the Wick product.

In this paper, we summarize the properties of the aforementioned two stochastic elliptic models and focus on a comparison study of Eqs. (1) and (2) subject to log-normal random coefficients $a(\boldsymbol{x},\omega)$. It is shown that these two models are only comparable when the degree of perturbation of $a(\boldsymbol{x},\omega)$ is $\ll 1$. The main difference between solutions of Eqs. (1) and (2) is characterized by a scaling factor, which is an exponential function of the degree of perturbation of $a(\boldsymbol{x},\omega)$. To eliminate such a scaling factor, we construct a new stochastic elliptic model, which is also based on the Wick product. This new model is highly comparable to model (I) for many cases. Furthermore, due to the Wick product, the new stochastic elliptic model can be approximated efficiently using the Wiener chaos expansion. The above observations will be demonstrated through a comparison study for a one-dimensional stochastic elliptic problem.

This paper is organized as follows. In Section 2 we introduce the Wiener chaos space. We present three stochastic elliptic models and compare them in Section 3. Numerical study is given in Section 4 followed by a summary section.

2. Wiener chaos space

We consider white noise defined on the space $L_2(D)$, where D indicates the physical domain. Let $\{\mathfrak{u}_k\}_{k=1}^{\infty}$ be a complete orthonormal basis of $L_2(D)$ and $\dot{W} = \{\dot{W}(h),\ h \in L_2(D)\}$ a zero-mean Gaussian family such that

$$\mathbb{E}[\dot{W}(h_1)\dot{W}(h_2)] = (h_1, h_2), \quad \forall h_1, h_2 \in L_2(D), \tag{3}$$

where $(\cdot,\cdot)$ indicates the inner product on $L_2(D)$. The (Gaussian) white noise is defined as the formal series

$$\dot{W} = \sum_k \dot{W}(\mathfrak{u}_k)\mathfrak{u}_k. \tag{4}$$

According to Eq. (3), one can verify that the mapping $h \to \dot{W}(h)$ is linear, which implies that $\{\dot{W}(h)\}$ is a Gaussian family. Due to the fact that $(\mathfrak{u}_i, \mathfrak{u}_j) = \delta_{ij}, \dot{W}(\mathfrak{u}_k) \sim \mathcal{N}(0,1)$ are independent normal random variables. Thus a formal series $\dot{W} = \sum_{k\geqslant 1}\xi_k\mathfrak{u}_k$ defines Gaussian *white noise* on $L_2(D)$, where $\xi_k \sim \mathcal{N}(0,1)$ are independent normal random variables. We then define $\mathbb{F} := (\Omega, \mathcal{F}, P)$ as a complete probability space, where $\mathcal{F}$ is the σ-algebra generated by the countably many i.i.d. Gaussian random variables $\{\xi_k\}_{k\geqslant 1}$. We define a random vector $\boldsymbol{\xi} := (\xi_1, \xi_2, \ldots)$.

Let $\mathcal{J}$ be the collection of multi-indices $\boldsymbol{\alpha}$ with $\boldsymbol{\alpha} = (\alpha_1, \alpha_2, \ldots)$ so that $\alpha_k \in \mathbb{N}_0$ and $|\boldsymbol{\alpha}| := \sum_{k\geqslant 1}\alpha_k < \infty$. For $\boldsymbol{\alpha}, \boldsymbol{\beta} \in \mathcal{J}$, we define

$$\boldsymbol{\alpha} + \boldsymbol{\beta} = (\alpha_1 + \beta_1, \alpha_2 + \beta_2, \ldots), \quad |\boldsymbol{\alpha}| = \sum_{k\geqslant 1}\alpha_k, \quad \boldsymbol{\alpha}! = \prod_{k\geqslant 1}\alpha_k!.$$

We use $(\mathbf{0})$ to denote the multi-index with all zero entries: $(\mathbf{0})_k = 0$ for all k. Define the collection of random variables $\Xi = \{h_{\boldsymbol{\alpha}}, \boldsymbol{\alpha} \in \mathcal{J}\}$ as follows:

$$h_{\boldsymbol{\alpha}}(\boldsymbol{\xi}) = \frac{1}{\sqrt{\boldsymbol{\alpha}!}}H_{\boldsymbol{\alpha}}(\boldsymbol{\xi}) = \prod_{k\geqslant 1}\frac{1}{\sqrt{\alpha_k!}}H_{\alpha_k}(\xi_k),$$

where $H_n(x)$ are one-dimensional Hermite polynomials of order n. For any fixed k, the following relation holds

$$\mathbb{E}[H_{\alpha_k}(\xi_k)H_{\beta_k}(\xi_k)] = \delta_{\alpha_k\beta_k}\alpha_k!, \quad \mathbb{E}[h_{\boldsymbol{\alpha}}h_{\boldsymbol{\beta}}] = \delta_{\boldsymbol{\alpha}\boldsymbol{\beta}}. \tag{5}$$

Recall the following result.

Theorem 2.1 [3]. *The set Ξ is an orthonormal basis in $L_2(\mathbb{F})$: if $\eta \in L_2(\mathbb{F})$ and $\eta_{\boldsymbol{\alpha}} = \mathbb{E}[\eta h_{\boldsymbol{\alpha}}]$, then $\eta = \sum_{\boldsymbol{\alpha}\in\mathcal{J}}\eta_{\boldsymbol{\alpha}}h_{\boldsymbol{\alpha}}$ and $\mathbb{E}[\eta^2] = \sum_{\boldsymbol{\alpha}\in\mathcal{J}}\eta_{\boldsymbol{\alpha}}^2$.*

Given a real separable Hilbert space X, we denote by $L_2(\mathbb{F};X)$ the Hilbert space of square-integrable $\mathcal{F}$-measurable X-valued random elements f. When $X = \mathbb{R}$, we write $L_2(\mathbb{F})$ instead of $L_2(\mathbb{F};\mathbb{R})$. Given a collection $\mathcal{R} = \{r_{\boldsymbol{\alpha}},\ \boldsymbol{\alpha} \in \mathcal{J}\}$ of uniformly bounded positive real numbers, we define the space $\mathcal{R}L_2(\mathbb{F};X)$ as the closure of $L_2(\mathbb{F};X)$ in the norm

$$\|u\|^2_{\mathcal{R}L_2(\mathbb{F};X)} = \sum_{\boldsymbol{\alpha}\in\mathcal{J}} r_{\boldsymbol{\alpha}}\|u_{\boldsymbol{\alpha}}\|_X^2, \tag{6}$$

where $u = \sum_{\boldsymbol{\alpha}\in\mathcal{J}}u_{\boldsymbol{\alpha}}h_{\boldsymbol{\alpha}}(\boldsymbol{\xi})$. The space $\mathcal{R}L_2(\mathbb{F};X)$ is called a weighted Wiener chaos space [9]. For the stochastic elliptic problems studied in this work, X is chosen as $H_0^1(D)$.

3. Three stochastic elliptic models

Let D be a bounded, connected, open subset of $\mathbb{R}^d$ $(d = 1, 2, 3)$ with a Lipschitz continuous boundary ∂D. The deterministic elliptic equation takes the form

$$\begin{cases} -\nabla\cdot(\hat{a}(\boldsymbol{x})\nabla u(\boldsymbol{x})) = f(\boldsymbol{x}), & \boldsymbol{x} \in D, \\ u(\boldsymbol{x}) = 0, & \boldsymbol{x} \in \partial D, \end{cases} \tag{7}$$

where $\hat{a}(\boldsymbol{x})$ indicates the effective coefficient. Eq. (7) is equivalent to the following first-order system

$$\begin{cases} \hat{a}(\boldsymbol{x})\nabla u(\boldsymbol{x}) = \boldsymbol{F}(\boldsymbol{x}), & \boldsymbol{x} \in D, \\ -\nabla\cdot\boldsymbol{F}(\boldsymbol{x}) = f(\boldsymbol{x}), & \boldsymbol{x} \in D, \\ u(\boldsymbol{x}) = 0, & \boldsymbol{x} \in \partial D. \end{cases} \tag{8}$$

In practice, it is more appropriate to replace the deterministic coefficient $\hat{a}(\boldsymbol{x})$ with a random process for many cases, such as in porous media, to take into account the randomness. Then we need to generalize (7) to be a stochastic PDE. Obviously the generalization is not unique due to different definitions of the stochastic integration. To this end, we consider the following general stochastic elliptic model:

$$\begin{cases} \nabla u(\boldsymbol{x},\omega) = Ta(\boldsymbol{x},\omega)\circ\boldsymbol{F}(\boldsymbol{x},\omega), & \boldsymbol{x} \in D, \\ -\nabla\cdot\boldsymbol{F}(\boldsymbol{x},\omega) = f(\boldsymbol{x}), & \boldsymbol{x} \in D, \\ u(\boldsymbol{x}) = 0, & \boldsymbol{x} \in \partial D. \end{cases} \tag{9}$$

where $a(\boldsymbol{x},\omega)$ is a random process, T indicates a proper map determined by a certain modeling strategy, '$\circ$' a proper operation, and $f(\boldsymbol{x})$ is assumed to be deterministic for simplicity. We also need the following positivity assumptions:

Assumption 3.1. There exists positive numbers λ_i and $\tilde{\lambda}_i$, $i = 1, 2$, such that

$$0 < \lambda_1 \leqslant \mathbb{E}[a](\boldsymbol{x}) \leqslant \lambda_2 < \infty, \quad 0 < \tilde{\lambda}_1 \leqslant \mathbb{E}[a^{-1}](\boldsymbol{x}) \leqslant \tilde{\lambda}_2 < \infty. \tag{10}$$

Example 3.2. Consider a log-normal random process $a(x,\omega) = e^{c+G(\boldsymbol{x},\omega)}$, where $G(\boldsymbol{x},\omega)$ is a *second-order* Gaussian random process with zero mean and c is constant. Then $\|\mathbb{E}[a](\boldsymbol{x})\|_{L^\infty(D)} < \infty$, and

$$\mathbb{E}[a^{-1}](\boldsymbol{x}) = e^{-c}\mathbb{E}[e^{-G(\boldsymbol{x},\omega)}] = e^{-c}\mathbb{E}[e^{G(\boldsymbol{x},\omega)}] = e^{-2c}\mathbb{E}[a](\boldsymbol{x}).$$

Thus, log-normal random processes satisfy our assumptions.

We now define the map T and operation $\circ$ in Eq. (9) as follows:

$$\begin{aligned}
&(\mathrm{I}): \ Ta(\boldsymbol{x},\omega) := a^{-1}(\boldsymbol{x},\omega), \quad \circ := \cdot,\\
&(\mathrm{II}): \ Ta(\boldsymbol{x},\omega) := a^{\diamondsuit(-1)}(\boldsymbol{x},\omega), \quad \circ := \diamondsuit,\\
&(\mathrm{III}): \ Ta(\boldsymbol{x},\omega) := a^{-1}(\boldsymbol{x},\omega), \circ := \diamondsuit,
\end{aligned}$$

where $\cdot$ indicates the regular product, and $\diamondsuit$ the Wick product defined as

$$H_{\boldsymbol{\alpha}}(\xi)\diamondsuit H_{\boldsymbol{\beta}}(\xi) = H_{\boldsymbol{\alpha}+\boldsymbol{\beta}}(\xi), \quad \forall \boldsymbol{\alpha}, \boldsymbol{\beta} \in \mathcal{J}, \tag{11}$$

and $a^{\diamondsuit(-1)}(\boldsymbol{x},\omega)$ is the inverse of $a(\boldsymbol{x},\omega)$ with respect to the Wick product satisfying

$$a(\boldsymbol{x},\omega)\diamondsuit a^{\diamondsuit(-1)}(\boldsymbol{x},\omega) = 1. \tag{12}$$

Proposition 3.3. *If Assumption 3.1 holds, then $a^{\diamondsuit(-1)}(\boldsymbol{x},\omega)$ exists.*

Proof. Let $a(\boldsymbol{x},\omega) = \sum_{\boldsymbol{\alpha}\in\mathcal{J}} a_{\boldsymbol{\alpha}}(\boldsymbol{x})H_{\boldsymbol{\alpha}}(\xi)$ and $a^{\diamondsuit(-1)}(\boldsymbol{x},\omega) = \sum_{\boldsymbol{\alpha}\in\mathcal{J}} \tilde{a}_{\boldsymbol{\beta}}(\boldsymbol{x})$-$H_{\boldsymbol{\beta}}(\xi)$. Substituting them into Eq. (12) and comparing the coefficients of $H_\alpha(\xi)$, we obtain

$$\tilde{a}_{(\mathbf{0})}(\boldsymbol{x}) = a^{-1}_{(\mathbf{0})}(\boldsymbol{x}), \quad \tilde{a}_{\boldsymbol{\alpha}}(\boldsymbol{x}) = -a^{-1}_{(\mathbf{0})}(\boldsymbol{x})\sum_{\boldsymbol{\beta}<\boldsymbol{\alpha}} a_{\boldsymbol{\alpha}-\boldsymbol{\beta}}(\boldsymbol{x})\tilde{a}_{\boldsymbol{\beta}}(\boldsymbol{x}). \tag{13}$$

Since $a_{(\mathbf{0})}(\boldsymbol{x}) = \mathbb{E}[a](\boldsymbol{x}) > 0$, the conclusion follows. □

If we consider the Wiener chaos expansion of $H_{\boldsymbol{\alpha}}(\xi)H_{\boldsymbol{\beta}}(\xi)$, it is obvious that there exist lower-order terms except for $H_{\boldsymbol{\alpha}+\boldsymbol{\beta}}(\xi)$; however, in the definition of Wick product, all these lower-order terms are removed. Such a difference between the Wick product and the regular product stems from the fact that the Wick product should be interpreted from the stochastic integral point of view. The connection of Wick product with Itô-Skorohod integral can be found in [7,11,9,18].

Corresponding to the three choices of T and $\circ$, we have the following three stochastic PDEs of elliptic type:

$$(\mathrm{I}): \ -\nabla\cdot(a(\boldsymbol{x},\omega)\nabla u_{\mathrm{I}}(\boldsymbol{x},\omega)) = f(\boldsymbol{x}), \tag{14}$$

$$(\mathrm{II}): \ -\nabla\cdot(a(\boldsymbol{x},\omega)\diamondsuit\nabla u_{\mathrm{II}}(\boldsymbol{x},\omega)) = f(\boldsymbol{x}), \tag{15}$$

$$(\mathrm{III}): \ -\nabla\cdot\left(\left(a^{-1}\right)^{\diamondsuit(-1)}(\boldsymbol{x},\omega)\diamondsuit\nabla u_{\mathrm{III}}(\boldsymbol{x},\omega)\right) = f(\boldsymbol{x}). \tag{16}$$

Models (I) and (II) correspond to Eqs. (1) and (2), respectively, while model (III) is a new stochastic elliptic model based on the Wick product. Obviously the three stochastic elliptic models are characterized by the different definitions of the fluxes:

$$\boldsymbol{F}_{\mathrm{I}} = a\nabla u_{\mathrm{I}}, \quad \boldsymbol{F}_{\mathrm{II}} = a\diamondsuit\nabla u_{\mathrm{II}}, \quad \nabla u_{\mathrm{III}} = a^{-1}\diamondsuit\boldsymbol{F}_{\mathrm{III}}. \tag{17}$$

In model (I), the flux is defined as a point-wise multiplication of $a(\boldsymbol{x},\omega)$ and ∇u_{I}; in model (II), the flux corresponds to a stochastic integral of $a(\boldsymbol{x},\omega)$ and ∇u_{II} through the Wick product; in model (III), ∇u_{III} corresponds to a similar stochastic integral of $a^{-1}(\boldsymbol{x},\omega)$ and $\boldsymbol{F}_{\mathrm{III}}(\boldsymbol{x},\omega)$. Roughly speaking, model (II) smooths the *flux* while model (III) smooths the *gradient*.

3.1. Mean solutions of models (I)–(III)

Let $a(\boldsymbol{x},\omega) = \mathbb{E}[a](\boldsymbol{x}) + \delta a(\boldsymbol{x},\omega)$ and $u_{\mathrm{I}}(\boldsymbol{x},\omega) = \mathbb{E}[u_{\mathrm{I}}](\boldsymbol{x}) + \delta u_{\mathrm{I}}(\boldsymbol{x},\omega)$, where δa and δu_{I} indicate the perturbations around the mean values of $a(\boldsymbol{x},\omega)$ and $u_{\mathrm{I}}(\boldsymbol{x},\omega)$. Then Eq. (14) can be rewritten as

$$\begin{aligned}
&-\nabla\cdot(\mathbb{E}[a]\nabla\mathbb{E}[u_{\mathrm{I}}]) - \nabla\cdot(\delta a\nabla\mathbb{E}[u_{\mathrm{I}}]) - \nabla\cdot(\mathbb{E}[a]\nabla\delta u_{\mathrm{I}}) - \nabla\cdot(\delta a\nabla\delta u_{\mathrm{I}})\\
&\quad = f(\boldsymbol{x}).
\end{aligned} \tag{18}$$

Taking the mean of the above equation, we obtain

$$-\nabla\cdot(\mathbb{E}[a]\nabla\mathbb{E}[u_{\mathrm{I}}]) - \nabla\cdot\mathbb{E}[\delta a\nabla\delta u_{\mathrm{I}}] = f(\boldsymbol{x}). \tag{19}$$

It is obvious that there does not exist explicitly an equation for $\mathbb{E}[u_{\mathrm{I}}](\boldsymbol{x})$ since we need the high-order moments $\nabla\cdot\mathbb{E}[\delta a\nabla\delta u_{\mathrm{I}}]$ for the closure, which are, in general, unknown and need more assumptions to be dealt with, such as in the homogenization theory. In other words, the effective coefficient $\hat{a}(\boldsymbol{x})$ for model (I) is usually not the same as $\mathbb{E}[a](\boldsymbol{x})$. However, both models (II) and (III) have a deterministic PDE for the mean solution. By taking the expectation of both sides of Eqs. (15) and (16), we obtain

$$-\nabla\cdot(\mathbb{E}[a](\boldsymbol{x})\cdot\nabla\mathbb{E}[u_{\mathrm{II}}](\boldsymbol{x})) = f(\boldsymbol{x}), \tag{20}$$

$$-\nabla\cdot\left(\frac{1}{\mathbb{E}[a^{-1}](\boldsymbol{x})}\cdot\nabla\mathbb{E}[u_{\mathrm{III}}](\boldsymbol{x})\right) = f(\boldsymbol{x}). \tag{21}$$

Since $\mathbb{E}[a](\boldsymbol{x})$ is positive, we can use it to define the energy norm

$$\|v\|_e = \left(\int_D \mathbb{E}[a](\boldsymbol{x})\nabla v\cdot\nabla v d\boldsymbol{x}\right)^{1/2}, \quad \forall v \in H^1_0(D). \tag{22}$$

Comparing Eq. (19) with Eq. (20), we see that the effect of the Wick product for the mean solution is equivalent to omitting the second-order perturbation term in Eq. (19), which implies that $\mathbb{E}[u_{\mathrm{I}}](\boldsymbol{x})$ and $\mathbb{E}[u_{\mathrm{II}}](\boldsymbol{x})$ are comparable only when the perturbation of $a(\boldsymbol{x},\omega)$ is very small and smooth.

We subsequently present some general properties of $\mathbb{E}[u_{\mathrm{II}}]$ and $\mathbb{E}[u_{\mathrm{III}}]$.

Proposition 3.4. $\|\mathbb{E}[u_{\mathrm{II}}]\|_e \leqslant \|\mathbb{E}[u_{\mathrm{III}}]\|_e$.

Proof. Considering the function t^{-1}, we have

$$\mathbb{E}[a](\boldsymbol{x}) \geqslant \frac{1}{\mathbb{E}[a^{-1}](\boldsymbol{x})}$$

from the Jensen's inequality. From Eqs. (20) and (21), we have

$$\int_D \mathbb{E}[a]\nabla\mathbb{E}[u_{\mathrm{II}}]\cdot\nabla v d\boldsymbol{x} = \int_D \frac{1}{\mathbb{E}[a^{-1}]}\nabla\mathbb{E}[u_{\mathrm{III}}]\cdot\nabla v d\boldsymbol{x}, \quad \forall v \in H^1_0(D). \tag{23}$$

Let $v = \mathbb{E}[u_{\mathrm{II}}]$. We obtain

$$\begin{aligned}
\|\mathbb{E}[u_{\mathrm{II}}]\|^2_e &= \int_D \mathbb{E}[a]\nabla\mathbb{E}[u_{\mathrm{II}}]\cdot\nabla\mathbb{E}[u_{\mathrm{II}}]\\
&= \int_D \frac{\frac{1}{\mathbb{E}[a^{-1}]}}{\mathbb{E}[a]}\mathbb{E}[a]\nabla\mathbb{E}[u_{\mathrm{III}}]\cdot\nabla\mathbb{E}[u_{\mathrm{II}}]d\boldsymbol{x} \leqslant \|\mathbb{E}[u_{\mathrm{III}}]\|_e\|\mathbb{E}[u_{\mathrm{II}}]\|_e,
\end{aligned} \tag{24}$$

which yields the conclusion. □

Proposition 3.5. *If Assumption 3.1 holds, then*

$$\lambda_1\tilde{\lambda}_1 \leqslant \frac{\|\mathbb{E}[u_{\mathrm{III}}]\|_{H^1_0(D)}}{\|\mathbb{E}[u_{\mathrm{II}}]\|_{H^1_0(D)}} \leqslant \lambda_2\tilde{\lambda}_2. \tag{25}$$

Proof. Substituting $v = \mathbb{E}[u_{\mathrm{II}}]$ into Eq. (23), we obtain

$$\lambda_1\|\mathbb{E}[u_{\mathrm{II}}]\|^2_{H^1_0(D)} \leqslant \frac{1}{\tilde{\lambda}_1}\|\mathbb{E}[u_{\mathrm{III}}]\|_{H^1_0(D)}\|\mathbb{E}[u_{\mathrm{II}}]\|_{H^1_0(D)},$$

which results in

$$\lambda_1\tilde{\lambda}_1\|\mathbb{E}[u_{\mathrm{II}}]\|_{H_0^1(D)} \leqslant \|\mathbb{E}[u_{\mathrm{III}}]\|_{H_0^1(D)}.$$

Similarly, we can let $v = \mathbb{E}[u_{\mathrm{III}}]$, which yields

$$\|\mathbb{E}[u_{\mathrm{III}}]\|_{H_0^1(D)} \leqslant \lambda_2\tilde{\lambda}_2\|\mathbb{E}[u_{\mathrm{II}}]\|_{H_0^1(D)}.$$

Combining the above two inequalities, we obtain the conclusion. □

3.2. Existence of solutions

We start with the uncertainty propagators of models (I)–(III). Assume that

$$a(\boldsymbol{x},\omega) = \sum_{\boldsymbol{\alpha}\in\mathcal{J}} a_{\boldsymbol{\alpha}}(\boldsymbol{x})H_{\boldsymbol{\alpha}}(\xi), \quad \left(a^{-1}(\boldsymbol{x},\omega)\right)^{\diamondsuit(-1)} = \sum_{\boldsymbol{\alpha}\in\mathcal{J}} \hat{a}_{\boldsymbol{\alpha}}(\boldsymbol{x})H(\xi). \tag{26}$$

Substituting the chaos expansions of u_{I}–u_{III} into Eqs. (14)–(16), respectively, and implementing the Galerkin projection in the probability space, we obtain the corresponding *uncertainty propagators* of models (I)–(III)

$$-\sum_{\boldsymbol{\alpha}\in\mathcal{J}} \nabla\cdot\left(\mathbb{E}[a(\boldsymbol{x},\omega)H_{\boldsymbol{\alpha}}H_{\gamma}]\nabla u_{\mathrm{I},\boldsymbol{\alpha}}(\boldsymbol{x})\right) = f(\boldsymbol{x})\delta_{(\mathbf{0}),\gamma}, \tag{27a}$$

$$-\sum_{\boldsymbol{\alpha}\leqslant\gamma} \nabla\cdot\left(a_{\gamma-\boldsymbol{\alpha}}(\boldsymbol{x})\nabla u_{\mathrm{II},\boldsymbol{\alpha}}(\boldsymbol{x})\right) = f(\boldsymbol{x})\delta_{(\mathbf{0}),\gamma}, \tag{27b}$$

$$-\sum_{\boldsymbol{\alpha}\leqslant\gamma} \nabla\cdot\left(\hat{a}_{\gamma-\boldsymbol{\alpha}}(\boldsymbol{x})\nabla u_{\mathrm{III},\boldsymbol{\alpha}}(\boldsymbol{x})\right) = f(\boldsymbol{x})\delta_{(\mathbf{0}),\gamma}, \tag{27c}$$

for any $\gamma\in\mathcal{J}$, which are high-dimensional deterministic partial differential equations. We note here that Eq. (27a) is a coupled system while Eqs. (27b) and (27c) are decoupled systems due to the lower-triangular structure, i.e., $u_{\mathrm{II},\gamma}$ and $u_{\mathrm{III},\gamma}$ only depend on the chaos coefficients $u_{\mathrm{II},\boldsymbol{\alpha}}$ and $u_{\mathrm{III},\boldsymbol{\alpha}}$, respectively, with $\boldsymbol{\alpha}<\gamma$.

For numerical computations, the truncation of $\{\xi_i\}$ and $\{h_{\boldsymbol{\alpha}}(\xi)\}$ is required. We usually choose the first M most important random dimensions of ξ and define the truncated Wiener chaos space as $\{h_{\boldsymbol{\alpha}} \mid \boldsymbol{\alpha}\in\mathcal{J}_{M,p}\}$, where $\boldsymbol{\alpha}\in\mathbb{N}_0^M$ and $|\boldsymbol{\alpha}|\leqslant p$ for any $\boldsymbol{\alpha}\in\mathcal{J}_{M,p}\subset\mathcal{J}$. The importance of each random dimension ξ_i usually depends on the correlation length and the regularity of the correlation functions of $a(\boldsymbol{x},\omega)$. For example, in the expression of Karhunen-Loève expansion of $a(\boldsymbol{x},\omega)$ (see Eq. (48)), M relies on the decay rate of the eigenvalues of the correlation function [5]. Uncertainty propagators (27a), (27b), (27c) can then be solved by any classical numerical methods for PDEs, such as finite element methods. For Eq. (27a), iterative methods, such as the block Gauss-Siedel method and the conjugate gradient method, are usually more efficient due to the coupling between coefficients $u_{\mathrm{I},\boldsymbol{\alpha}}$. The efficiency of such iterative methods relies heavily on the degree of perturbation of $a(\boldsymbol{x},\omega)$, in other words, a good preconditioner is usually necessary for approximating Eq. (27a). For Eqs. (27b) and (27c), the coefficients $u_{\mathrm{II},\boldsymbol{\alpha}}$ and $u_{\mathrm{III},\boldsymbol{\alpha}}$ can be solved one-by-one, which can be very efficient. We refer to [1,5,17,16,18,10] for more details about the accuracy and efficiency of the stochastic finite element methods for models (I) and (II).

We subsequently summarize some theoretical results for models (I) and (II) with $a(\boldsymbol{x},\omega)$ being a log-normal random process. Results are mainly from [13] for model (I), and [10] for model (II). Since both models (II) and (III) are based on the Wick product, all the results for model (II) can be adapted for model (III).

A lot of work on numerical analysis for model (I) has been done (see [1,2,5,6] and references therein). Most of the work is based on the assumption of strong ellipticity, which means that the coefficient $a(\boldsymbol{x},\omega)$ is positive and uniformly bounded from below. Obviously this assumption is too strong for the log-normal random processes. Recently the numerical analysis of stochastic finite element method for model (I) with $a(\boldsymbol{x},\omega)$ being log-normal was carried out in [13], which is based on white noise analysis and weighted L_2 norm in the probability space, since the regular L_2 norm is not enough for the convergence study due to the relaxation of the uniform ellipticity. Instead of using the probability space $\mathbb{F} = (\Omega,\mathcal{F},P)$, which is generated by countably many i.i.d. normal random variables, the white noise analysis uses the probability space $\hat{\mathbb{F}} = (\mathcal{S}',\mathcal{B}(\mathcal{S}'),\mu)$, where $\mathcal{S}'$ is a properly defined space of distributions, $\mathcal{B}(\mathcal{S}')$ is the σ-field of Borel subsets of $\mathcal{S}'$, and μ is the white noise measure given by the Bochner-Minlos theorem

$$\mathbb{E}[e^{i\langle\cdot,\phi\rangle}] := \int_{\mathcal{S}'} e^{i\langle w,\phi\rangle}d\mu(w) = e^{-\frac{1}{2}\|\phi\|_2^2}, \quad \forall\phi\in\mathcal{S}. \tag{28}$$

With $\mathcal{S}'$ being the dual of $\mathcal{S}$, $\langle w,\phi\rangle = w(\phi)$ is the action of w on ϕ. A general definition of $\mathcal{S}$ can be found in [13].

The coefficients $a(\boldsymbol{x},\omega)$ is modeled as $a(\boldsymbol{x},\omega) := e^{W_\phi(\boldsymbol{x},w)}$, where $W_\phi(\boldsymbol{x},w)$ is the smoothed white noise (see Section 3.3) defined as $W_\phi(x,w) := \langle w,\phi_{\boldsymbol{x}}\rangle$ with $\phi_{\boldsymbol{x}}\in L_2(D)$ and $w\in\mathcal{S}'$. To study the stochastic elliptic problem

$$-\nabla\cdot(e^{W_\phi(\boldsymbol{x},w)}\nabla u_{\mathrm{I}}) = f(\boldsymbol{x}), \tag{29}$$

we define V_s as the weighted space consisting of functions $v: D\times\mathcal{S}'\to\mathbb{R}$ such that

$$\|v\|_{V_s}^2 := \int_{\mathcal{S}'}\|v\|_{H_0^1(D)}^2 e^{s\|w\|_{-\theta}^2}d\mu(w) < \infty, \quad s\in\mathbb{R}, \tag{30}$$

and its dual as

$$V_{-s} := \{v(w) \mid \|v\|_{V_{-s}}^2 = \int_{\mathcal{S}'}\|v\|_{H_0^1(D)}^2 e^{-s\|w\|_{-\theta}^2}d\mu(w) < \infty\}. \tag{31}$$

Then the following inf–sup condition holds

Theorem 3.6. [13]. *Let $\epsilon > 0$ and assume that $C_\theta = \sup_{x\in D}\|\phi_x\|_\theta < \infty$. Then the bilinear form $a(\cdot,\cdot): V_s\times V_{-s+\epsilon}\to\mathbb{R}$ given by Eq. (29) is continuous and bounded, i.e.*

$$a(u,v) \leqslant e^{\frac{C_\theta^2}{2\epsilon}}\|u\|_{V_s}\|v\|_{V_{-s+\epsilon}}, \tag{32}$$

and satisfies the following inf–sup condition

$$\inf_{u\in V_s\setminus\{0\}}\sup_{v\in V_{-s-\epsilon}\setminus\{0\}}\frac{a(u,v)}{\|u\|_{V_s}\|v\|_{V_{-s-\epsilon}}} \geqslant e^{-\frac{C_\theta}{2\epsilon}}. \tag{33}$$

For $f\in V'_{-s-\epsilon}\subset V'_{-s+\epsilon}$, there exists a unique solution $u_I\in V_s$ satisfying the weak form

$$a(u_{\mathrm{I}},v) = \langle f,v\rangle, \quad \forall v\in V_{-s+\epsilon}. \tag{34}$$

Note here that we need the constant ϵ to be positive. If $u_{\mathrm{I}}\in V_0$, we need $f\in V'_{-\epsilon}$. If $f\in V'_0$, we have $u_{\mathrm{I}}\in V_{-\epsilon}$, in other words, we must associate u_{I} to a weight $e^{-\epsilon\|w\|_{-\theta}^2}$ in the probability space $\hat{\mathbb{F}}$. Based on Theorem 3.6, the convergence of a stochastic finite element method can be established. Note here that with respect to the Winer chaos, a proper set $\mathcal{R} = \{r_{\boldsymbol{\alpha}},\boldsymbol{\alpha}\in\mathcal{J}\}$ of uniformly bounded positive real numbers can be defined according to the weight $e^{s\|w\|_{-\theta}^2}$, which establishes a correspondence between V_s and the weighted Wiener chaos space $\mathcal{R}L_2(\mathbb{F};H_0^1(D))$, see Eq. (6).

Numerical analysis for model (II) was implemented in [17,16] using the white noise analysis. We here discuss it in the weighted Wiener chaos space, which takes advantage of the lower-triangular structure of the uncertainty propagator [9,18,10]. Eqs. (27b) and (27c) have the same abstract form

$$\begin{cases} A_{(\mathbf{0})}u_{(\mathbf{0})} = f, & |\gamma| = 0,\\ A_{(\mathbf{0})}u_{\gamma} = -\sum\limits_{\substack{\boldsymbol{\alpha}\in\mathcal{J}\\ 0<\boldsymbol{\alpha}\leqslant\gamma}} A_{\boldsymbol{\alpha}}u_{\gamma-\boldsymbol{\alpha}}, & |\gamma| > 0, \end{cases} \tag{35}$$

where we neglect the subscripts II and III, and $A_{\boldsymbol{\alpha}} = -\nabla\cdot(a_{\boldsymbol{\alpha}}(\boldsymbol{x})\nabla)$. Then Eq. (35) can be solved as

$$\begin{cases} u_{(\mathbf{0})} = A_{(\mathbf{0})}^{-1} f, & |\boldsymbol{\gamma}| = 0, \\ u_{\boldsymbol{\gamma}} = -\sum\limits_{\substack{\boldsymbol{\alpha}\in\mathcal{J} \\ 0<\boldsymbol{\alpha}\leqslant\boldsymbol{\gamma}}} A_{(\mathbf{0})}^{-1} A_{\boldsymbol{\alpha}} u_{\boldsymbol{\gamma}-\boldsymbol{\alpha}}, & |\boldsymbol{\gamma}| > 0, \end{cases} \tag{36}$$

If operators $A_{(\mathbf{0})}^{-1}$ and $A_{(\mathbf{0})}^{-1} A_{\boldsymbol{\alpha}}$ are bounded, we can always find proper weights $\{r_{\boldsymbol{\alpha}}\}$ to construct a weighted Wiener chaos space $\mathcal{R}L_2(\mathbb{F}; H_0^1(D))$, in which a unique solution of Eq. (35) exists. Such observations are summarized in the following theorem

Theorem 3.7 [10]. *Assume that operators $A_{(\mathbf{0})}^{-1}$ and $A_{(\mathbf{0})}^{-1}A_{\boldsymbol{\alpha}}$, $\boldsymbol{\alpha}\in\mathcal{J}$, $|\boldsymbol{\alpha}|>0$, are bounded, where $\|A_{(\mathbf{0})}^{-1}A_{\boldsymbol{\alpha}}\|\leqslant C_{\boldsymbol{\alpha}}$. Let $b=(b_1,b_2,\ldots)$ be of sequence of positive numbers, such that $C_\alpha\leqslant b^\alpha$. Then* Eq. (35) *has a unique solution $u\in\mathcal{R}L_2(\mathbb{F};H_0^1(D))$ with weights $r_{\boldsymbol{\alpha}}=\frac{c^{\boldsymbol{\alpha}}}{\boldsymbol{\alpha}!}$ for a deterministic function $f(x)\in H^{-1}(D)$, where $c=(c_1, c_2,\ldots)$ is a sequence of positive numbers.*

Note that in Theorem 3.7, we do not assume explicitly that the random field $a(\boldsymbol{x},\omega)$ is log-normal as we do in Theorem 3.6. The assumptions in Theorem 3.7 are much more general and cover a relatively large class of nonlinear random coefficients with high-order Wiener chaos expansions, including the log-normal random fields.

3.3. Smoothed white noise

We subsequently consider the solution behavior of models (I)–(III), where $a(\boldsymbol{x},\omega)$ is a log-normal random process. We start from the definition of smoothed white noise [7]

$$W_\phi(\boldsymbol{x}) := \sum_{k\geqslant 1}(\phi_{\boldsymbol{x}}, u_k)\xi_k, \tag{37}$$

where $\phi_{\boldsymbol{x}}\in L_2(D)$. For example, let $\phi(\boldsymbol{y}) = \mathbb{I}_{[0,h]\times[0,h]}(\boldsymbol{y})$, where h is a positive number and $\mathbb{I}(\boldsymbol{y})$ is the indicator function. We can define $\phi_{\boldsymbol{x}} = \phi(\boldsymbol{y}-\boldsymbol{x})$. Obviously, $W_\phi(\boldsymbol{x})$ is a Gaussian random process. Note that this is a simple and direct way to introduce correlation. Obviously, $W_\phi(\boldsymbol{x}_1)$ and $W_\phi(\boldsymbol{x}_2)$ are correlated if $\boldsymbol{x}_2-\boldsymbol{x}_1$ or $\boldsymbol{x}_1-\boldsymbol{x}_2\in[0,h]\times[0,h]$, which introduces a correlation length h.

Let $a(\boldsymbol{x},\omega)=e^{\diamondsuit W_\phi(\boldsymbol{x})}$, where the Wick exponential is defined as

$$e^{\diamondsuit W_\phi(\boldsymbol{x})} = \sum_{n=0}^{\infty}\frac{1}{n!}W_\phi^{\diamondsuit n}(\boldsymbol{x}). \tag{38}$$

It can be readily checked that [7]

$$e^{\diamondsuit W_\phi(\boldsymbol{x})} = e^{W_\phi(\boldsymbol{x})-\frac{1}{2}\|\phi\|_2^2}, \tag{39}$$

and the following statistics hold

$$\mathbb{E}\left[e^{\diamondsuit W_\phi(\boldsymbol{x})}\right] = 1, \quad \mathrm{Var}\left(e^{\diamondsuit W_\phi(\boldsymbol{x})}\right) = e^{\|\phi\|_2^2}-1. \tag{40}$$

We also have

$$e^{\diamondsuit W_\phi(\boldsymbol{x})}\diamondsuit e^{\diamondsuit(-W_\phi(\boldsymbol{x}))} = 1. \tag{41}$$

For the one-dimensional case, we have the following exact solutions of u_i [7], i = I, II, III.

Theorem 3.8. *Let $L\in\mathbb{R}$, $D=(0,L)$, $a(x,\omega)=e^{\diamondsuit W_\phi(x)}$, and $f(x)\in L_1(D)$ is a deterministic function. Then the exact solutions of models (I)–(III) are:*

$$\begin{aligned} u_{\mathrm{I}} &= e^{\|\phi\|_2^2}\left\{\widetilde{A}\cdot\int_0^x e^{\diamondsuit(-W_\phi(t))}dt - \int_0^x\int_0^t f(s)ds e^{\diamondsuit(-W_\phi(t))}dt\right\}, \\ u_{\mathrm{II}} &= A\diamondsuit\int_0^x e^{\diamondsuit(-W_\phi(t))}dt - \int_0^x\int_0^t f(s)ds e^{\diamondsuit(-W_\phi(t))}dt, \\ u_{\mathrm{III}} &= e^{\|\phi\|_2^2}u_{\mathrm{II}}, \end{aligned} \tag{42}$$

where

$$\widetilde{A} = \left(\int_0^L e^{\diamondsuit(-W_\phi(t))}dt\right)^{-1}\cdot\int_0^L\int_0^t f(s)ds e^{\diamondsuit(-W_\phi(t))}dt,$$

$$A = \left(\int_0^L e^{\diamondsuit(-W_\phi(t))}dt\right)^{\diamondsuit(-1)}\diamondsuit\int_0^L\int_0^t f(s)ds e^{\diamondsuit(-W_\phi(t))}dt.$$

Proof. From Eq. (39), we have

$$\frac{1}{e^{\diamondsuit W_\phi(x)}} = e^{\frac{1}{2}\|\phi\|_2^2}e^{-W_\phi(x)} = e^{\|\phi\|_2^2}e^{\diamondsuit(-W_\phi(x))}.$$

Thus,

$$\left(\frac{1}{e^{\diamondsuit W_\phi(x)}}\right)^{\diamondsuit(-1)} = e^{-\|\phi\|_2^2}e^{\diamondsuit W_\phi(x)}, \tag{43}$$

where Eq. (41) is applied. Then we can follow the proof of theorem 4.6.2 in [7]. For completeness, we give a brief deviation for u_{II}. We consider

$$(e^{\diamondsuit W_\phi(x)}\diamondsuit u_{\mathrm{II}}'(x))' = -f(x),$$

subject to homogeneous boundary conditions on $[0, L]$, where $'$ indicate derivative with respect to x. Integrating the above equation, we obtain

$$e^{\diamondsuit W_\phi(x)}\diamondsuit u_{\mathrm{II}}'(x) = -\int_0^x f(t)dt + A(\omega),$$

where $A(\omega)$ is independent of x. Multiplying $e^{\diamondsuit(-W_\phi(x))}$ to both sides of the above equation with respect to Wick product and integrating it, we have

$$u_{\mathrm{II}}(x) = A(\omega)\diamondsuit\int_0^x e^{\diamondsuit(-W_\phi(t))}dt - \int_0^x\int_0^t f(s)ds e^{\diamondsuit(-W_\phi(t))}dt.$$

Using the boundary condition $u_{\mathrm{II}}(L)=0$, the random variable $A(\omega)$ can be determined. □

Remark 3.9. For a high-dimensional problem, no exact solution is available for model (I) while the exact solutions of model (II) and (III) can be obtained [7]. When $a(\boldsymbol{x},\omega)=e^{\diamondsuit W_\phi(\boldsymbol{x})}$, the relation $u_{\mathrm{III}}=e^{\|\phi\|_2^2}u_{\mathrm{II}}$ still holds due to the relation (43).

Based on the exact solution, it is easy to show that u_{I} for the one-dimensional problem is square integrable in the probability space by noting the fact

$$\begin{aligned} &\mathbb{E}\left[\left(\int_0^x g(t)e^{\diamondsuit(-W_\phi(t))}dt\right)^n\right] \\ &\quad\leqslant \mathbb{E}\left[x^{n-1}\int_0^x g^n(t)e^{-nW_\phi(t)-\frac{1}{2}n\|\phi\|_2^2}dt\right] \\ &\quad= x^{n-1}\int_0^x g^n(t)\mathbb{E}\left[e^{-nW_\phi(t)-\frac{1}{2}n\|\phi\|_2^2}\right]dt \\ &\quad= x^{n-1}e^{\frac{n^2}{2}\|\phi\|_2^2-\frac{1}{2}n\|\phi\|_2^2}\int_0^x g^n(t)dt<\infty, \quad \forall n\in\mathbb{Z}, \end{aligned} \tag{44}$$

where we assume that $g(t)$ is a positive function and $\int_0^x g^n(t)\,dt$ exists. For u_{I}, $g(t)=1$ or $|\int_0^t f(s)\,dt|$. In the above deviation, we employ the Jensen's inequality using the fact that x^n is convex for $n\in\mathbb{Z}$ on the interval $(0, +\infty)$. Thus, we can apply the Hölder inequality to the exact solution of u_{I} to show that u_{I} is square integrable for any x provided that $f(s)$ is good enough. Using Eq. (44) it can also be shown that for any x, both u_{II} and u_{III} are square integrable [7] in the probability space.

We now compare the exact solutions u_{I}, u_{II} and u_{III}. First, it is seen that the form of u_{I} is very similar to that of u_{III}. We can obtain u_{III} from u_{I} by replacing some multiplication operations $\cdot$ by Wick

product $\diamondsuit$. Second, compared to u_{I} and u_{III}, u_{II} does not have the scaling factor $e^{\|\phi\|_2^2}$, which is also the only difference between u_{II} and u_{III}. Thus, existence of the scaling factor should be related to the way that we apply the Wick product, see (9). Third, the scaling factor is an exponential function of $\|\phi\|_2^2$. We will show later on in Section 3.3.2 that $\|\phi\|_2^2$ can be related to the variance of $W_\phi(x)$. In other words, if the degree of perturbation of $a(x,\omega)$ increases, the difference between the statistics given by u_{I} and u_{II} will increase exponentially. Since u_{III} also includes the scaling factor $e^{\|\phi\|_2^2}$, we are more interested in the difference between u_{I} and u_{III}.

3.3.1. Spatially-independent noise

This is the simplest case, where $W_\phi(\boldsymbol{x})$ is independent of $\boldsymbol{x}$. Let $a(\boldsymbol{x},\omega) = e^{\sigma\xi-\frac{1}{2}\sigma^2}$, where $\xi\sim\mathcal{N}(0,1)$ and c is constant. In other words, we take $\phi(\boldsymbol{y})$ as a constant to smooth the white noise, see Eq. (37). It is easy to verify that

$$e^{\sigma\xi-\frac{1}{2}\sigma^2}\diamondsuit e^{-\sigma\xi-\frac{1}{2}\sigma^2} = 1. \tag{45}$$

Then the exact solutions of models (I)–(III) can be expressed as

$$u_{\mathrm{I}}(\boldsymbol{x},\omega) = e^{-\sigma\xi+\frac{1}{2}\sigma^2}\Delta^{-1}f(\boldsymbol{x}),$$
$$u_{\mathrm{II}}(\boldsymbol{x},\omega) = e^{-\sigma\xi-\frac{1}{2}\sigma^2}\Delta^{-1}f(\boldsymbol{x}),$$
$$u_{\mathrm{III}}(\boldsymbol{x},\omega) = e^{-\sigma\xi+\frac{1}{2}\sigma^2}\Delta^{-1}f(\boldsymbol{x}),$$

where Δ^{-1} is the inverse of Laplace operator satisfying the homogeneous boundary conditions. It is seen that models (I) and (III) give the same solutions for space-independent noise, while there exists a scaling factor $u_{\mathrm{I}}/u_{\mathrm{II}} = e^{\sigma^2}$ between models (I) and (II). Since

$$\mathbb{E}\left[e^{\sigma\xi-\frac{1}{2}\sigma^2}\right] = 1 \quad\text{and}\quad \mathrm{Var}\left(e^{\sigma\xi-\frac{1}{2}\sigma^2}\right) = e^{\sigma^2}-1,$$

the scaling factor increases exponentially with the degree of perturbation of $a(\boldsymbol{x},\omega)$.

3.3.2. Spatially-dependent noise

Let the smoothed white noise be a zero-mean stationary Gaussian process with a correlation function $R(\boldsymbol{x},\boldsymbol{y}) = R(\boldsymbol{x}-\boldsymbol{y})$. According to the Mercer theorem [15] we have

$$R(\boldsymbol{x},\boldsymbol{y}) = \sum_{i=1}^{\infty}\lambda_i\phi_i(\boldsymbol{x})\phi_i(\boldsymbol{y}), \tag{46}$$

where $\{\lambda_i,\phi_i(\boldsymbol{x})\}_{i=1}^{\infty}$ are eigen-pairs satisfying

$$\int_D R(\boldsymbol{x},\boldsymbol{y})\phi_i(\boldsymbol{x})d\boldsymbol{x} = \lambda_i\phi_i(\boldsymbol{y}), \quad \int_D \phi_i(\boldsymbol{x})\phi_j(\boldsymbol{x})d\boldsymbol{x} = \delta_{ij}. \tag{47}$$

Let $\phi_{\boldsymbol{x}} = \sum_{i=1}^{\infty}\sqrt{\lambda_i}\phi_i(\boldsymbol{x})\phi_i(\boldsymbol{y})$ and $\mathrm{u}_i = \phi_i(\boldsymbol{y})$. From Eq. (37), we obtain

$$W_\phi(\boldsymbol{x}) = \sum_{i=1}^{\infty}\sqrt{\lambda_i}\phi_i(\boldsymbol{x})\xi_i, \tag{48}$$

which is exactly the Karhunen-Loève expansion of the Gaussian random process. We also have

$$\|\phi_{\boldsymbol{x}}\|_2^2 = \sum_{i=1}^{\infty}\lambda_i\phi_i(\boldsymbol{x})\phi_i(\boldsymbol{x}) = R(0), \tag{49}$$

which is valid for any given $\boldsymbol{x}\in D$. Note that $R(0)$ is the variance of $W_\phi(\boldsymbol{x})$. We choose the above particular forms of $\phi_{\boldsymbol{x}}$ and u_i mainly due to the convenience for numerical computation. We now look at the Wiener chaos expansion of $e^{\diamondsuit W_\phi(\boldsymbol{x})}$. Using Eqs. (48) and (49), and the generating function of Hermite polynomials

$$e^{sx-\frac{1}{2}s^2} = \sum_{n=0}^{\infty}\frac{s^n}{n!}H_n(x), \tag{50}$$

we obtain

$$e^{\diamondsuit W_\phi(\boldsymbol{x})} = e^{W_\phi(\boldsymbol{x})-\frac{1}{2}\|\phi\|_2^2} = e^{\sum_{i=1}^{\infty}\sqrt{\lambda_i}\phi_i(\boldsymbol{x})\xi_i-\frac{1}{2}\lambda_i\phi_i(\boldsymbol{x})\phi_i(\boldsymbol{x})}$$
$$= \sum_{\boldsymbol{\alpha}\in\mathcal{J}}\frac{\Phi^{\boldsymbol{\alpha}}(\boldsymbol{x})}{\sqrt{\boldsymbol{\alpha}!}}h_{\boldsymbol{\alpha}}(\xi), \tag{51}$$

where

$$\Phi(\boldsymbol{x}) = \left(\sqrt{\lambda_1}\phi_1(\boldsymbol{x}),\sqrt{\lambda_2}\phi_2(\boldsymbol{x}),\ldots\right). \tag{52}$$

Example 3.10. It is known that the eigen-pairs $\{\lambda_i,\phi_i(x)\}$ for the one-dimensional exponential kernel $e^{-\frac{|x-y|}{l}}$ have the following analytical forms on $[0,L]$ [8]

$$\phi_i(x) = \frac{\hat{\lambda}_i l\cos(\hat{\lambda}_i x)+\sin(\hat{\lambda}_i x)}{\sqrt{\frac{1}{2}(1+\hat{\lambda}_i^2 l^2)L+(\hat{\lambda}_i^2 l^2-1)\frac{\sin(2\hat{\lambda}_i L)}{4\hat{\lambda}_i}+\frac{1}{2}l(1-\cos(2\hat{\lambda}_i L))}}, \tag{53}$$

where $\hat{\lambda}_i$ satisfying

$$\hat{\lambda}_i^2 = \frac{2/l-\lambda_i/l^2}{\lambda_i}, \quad (\hat{\lambda}_i^2-1/l^2)\tan(\hat{\lambda}_i T)-2\hat{\lambda}_i/l = 0. \tag{54}$$

We will use these formulas for numerical experiments in Section 4.

We subsequently present a numerical procedure to compute the statistics of u_{I}, u_{II} and u_{III} based on the exact solutions given in Theorem 3.8. A general numerical procedure is to solve the uncertainty propagators (27a)–(27c). Since the difference between u_{II} and u_{III} is just a scaling factor. We only consider u_{I} and u_{III}. Assume that

$$u_{\mathrm{I}}(x,\omega) = \sum_{\boldsymbol{\alpha}\in\mathcal{J}}u_{\mathrm{I},\boldsymbol{\alpha}}(x)h_{\boldsymbol{\alpha}}(\xi), \quad u_{\mathrm{III}}(x,\omega) = \sum_{\boldsymbol{\alpha}\in\mathcal{J}}u_{\mathrm{III},\boldsymbol{\alpha}}(x)h_{\boldsymbol{\alpha}}(\xi),$$
$$\int_0^x e^{\diamondsuit(-W_\phi)}dt = \sum_{\boldsymbol{\alpha}\in\mathcal{J}}g_{\boldsymbol{\alpha}}(x)h_{\boldsymbol{\alpha}}(\xi),$$

and

$$\int_0^x\int_0^t f(s)ds e^{\diamondsuit(-W_\phi)}dt = \sum_{\boldsymbol{\alpha}\in\mathcal{J}}\hat{g}_{\boldsymbol{\alpha}}(x)h_{\boldsymbol{\alpha}}(\xi),$$

where

$$g_{\boldsymbol{\alpha}}(x) = \int_0^x\frac{\Phi^{\boldsymbol{\alpha}}(t)}{\sqrt{\boldsymbol{\alpha}!}}dt, \quad \hat{g}_{\boldsymbol{\alpha}}(x) = \int_0^x\int_0^t f(s)ds\frac{\Phi^{\boldsymbol{\alpha}}(t)}{\sqrt{\boldsymbol{\alpha}!}}dt.$$

Using the Galerkin projection in the probability space, we then have

$$\sum_{\boldsymbol{\alpha},\boldsymbol{\beta}\in\mathcal{J}}u_{\mathrm{I},\boldsymbol{\alpha}}(x)g_{\boldsymbol{\beta}}(L)\mathbb{E}[h_{\boldsymbol{\alpha}}h_{\boldsymbol{\beta}}h_{\boldsymbol{\gamma}}]$$
$$= e^{\sigma^2}\sum_{\boldsymbol{\alpha},\boldsymbol{\beta}\in\mathcal{J}}\left(\hat{g}_{\boldsymbol{\alpha}}(L)g_{\boldsymbol{\beta}}(x)-g_{\boldsymbol{\alpha}}(L)\hat{g}_{\boldsymbol{\beta}}(x)\right)\mathbb{E}[h_{\boldsymbol{\alpha}}h_{\boldsymbol{\beta}}h_{\boldsymbol{\gamma}}], \tag{55}$$

and

$$\sum_{\boldsymbol{\alpha}\leqslant\boldsymbol{\gamma}}u_{\mathrm{III},\boldsymbol{\alpha}}(x)g_{\boldsymbol{\gamma}-\boldsymbol{\alpha}}(b)\binom{\boldsymbol{\gamma}}{\boldsymbol{\alpha}}^{1/2}$$
$$= e^{\sigma^2}\sum_{\boldsymbol{\alpha}\leqslant\boldsymbol{\gamma}}\left(\hat{g}_{\boldsymbol{\alpha}}(L)g_{\boldsymbol{\gamma}-\boldsymbol{\alpha}}(x)-g_{\boldsymbol{\alpha}}(L)\hat{g}_{\boldsymbol{\gamma}-\boldsymbol{\alpha}}(x)\right)\binom{\boldsymbol{\gamma}}{\boldsymbol{\alpha}}^{1/2}, \tag{56}$$

for any $\boldsymbol{\gamma}\in\mathcal{J}$, where $\sigma = \|\phi_x\|_2$. Noticing the fact that

$$h_i(\xi)h_j(\xi) = \sum_{k\leqslant i\wedge j}B(i,j,k)h_{i+j-2k}(\xi) \tag{57}$$

for one-dimensional normalized Hermite polynomials, where

$$B(i,j,l) = \left[\binom{i}{l}\binom{j}{l}\binom{i+j-2l}{i-l}\right]^{1/2},$$

we have

$$\mathbb{E}[h_{\boldsymbol{\alpha}} h_{\boldsymbol{\beta}} h_{\boldsymbol{\gamma}}] = \sum_{\boldsymbol{\kappa} \leqslant \boldsymbol{\alpha} \wedge \boldsymbol{\beta}} \mathbf{B}(\boldsymbol{\alpha}, \boldsymbol{\beta}, \boldsymbol{\kappa}) \delta_{\boldsymbol{\kappa}, \boldsymbol{\gamma}}, \quad \mathbf{B}(\boldsymbol{\alpha}, \boldsymbol{\beta}, \boldsymbol{\kappa}) = \prod_{i=1}^{\infty} B(\alpha_i, \beta_i, \kappa_i), \tag{58}$$

for the multi-dimensional cases. We note that for any given x, the linear system (55) for $u_{\mathrm{I}, \boldsymbol{\alpha}}$ is full while the linear system (56) for $u_{\mathrm{III}, \boldsymbol{\alpha}}$ is lower-triangular.

4. Numerical experiments

In this section, we study models (I)–(III) numerically. We will focus on the comparability of the statistics of u_{I}–u_{III} given in Theorem 3.8. Assume that the random coefficient $a(x, \omega) = e^{\diamond W_\phi(x)}$ is a log-normal random field, where the underlying Gaussian field $W_\phi(x)$ is subject to an exponential correlation function $R(x-y) = \sigma^2 e^{-\frac{|x-y|}{l}}$, where σ is the standard deviation of $W_\phi(x)$ and l the correlation length. The physical domain is $D = [0, 1]$ and $f(x) = 1$.

We first look at a relatively large correlation length $l = 5$ compared to the physical domain. We use four Gaussian random variables to approximate the underlying Gaussian random process (smoothed white noise) based on the Karhunen-Loève expansion

$$W_\phi(x) = \sum_{i=1}^{4} \sqrt{\lambda_i} \phi_i(x) \xi_i,$$

where λ_i and $\phi_i(x)$ are given by Eqs. (53) and (54). The smallest eigenvalue is 0.48% of the largest one. Since

$$\mathbb{E}\left[e^{\diamond W_\phi(x)}\right] = 1 \quad \text{and} \quad \mathrm{Var}\left(e^{\diamond W_\phi(x)}\right) = e^{\sigma^2} - 1,$$

σ can also indicate the degree of perturbation of $e^{\diamond W_\phi(x)}$. We then approximate the exact solutions given in Theorem 3.8 using fourth-order Wiener chaos. In Fig. 1 we plot the mean and the standard deviation of u_i, i = I, II, III, when $\sigma = 1$. We note that $\sigma = 1$ corresponds to a degree of perturbation around 130%. It can be seen that without the scaling factor $e^{\|\phi\|_2^2} = e^{\sigma^2}$, there exist a large difference between statistics of u_{I} and u_{II}. However, the corresponding statistics of u_{I} and u_{III} are comparable. In Fig. 2, we plot the statistics of u_{I}, u_{II} and u_{III} at $x = 0.5$, where the largest standard deviation occurs. It is seen that the relative difference between the statistics increases with the degree of perturbations. When $\sigma = 1$ the relative difference between the statistics of u_{I} and u_{III} is 4.34% and 3.42% for the mean and the standard deviation, respectively.

We subsequently look at a smaller correlation length $l = 1$, which is still comparable with respect to the physical domain. We use eight random variables to construct the K–L expansion of $W_\phi(x)$. The smallest eigenvalue is 0.55% of the largest one. Fourth-order Wiener chaos expansions are employed. In Fig. 3, we plot the mean and the standard deviation at $x = 0.5$ with respect to the parameter σ. It can be seen that the difference between the statistics of u_{I} and u_{III} becomes larger as the correlation length l becomes smaller. When $\sigma = 1$, the relative difference between the statistics of u_{I} and u_{III} is 14.98% and 13.97% for the mean and standard deviation, respectively.

To this end, for a Gaussian random process $W_\phi(x)$ with a correlation function $R(x, y) = \sigma^2 e^{-\frac{|x-y|}{l}}$, we see that $\mathbb{E}[u_{\mathrm{I}}]$ depends on σ and l; $\mathbb{E}[u_{\mathrm{II}}]$ is independent of σ and l because only $\mathbb{E}[e^{\diamond W_\phi}] = 1$ is needed for Eq. (20) satisfied by $\mathbb{E}[u_{\mathrm{II}}]$; $\mathbb{E}[u_{\mathrm{III}}]$ only depends on σ since $u_{\mathrm{III}} = e^{\sigma^2} u_{\mathrm{II}}$. Furthermore, the dependence of $\mathbb{E}[u_{\mathrm{III}}]$ on σ is through

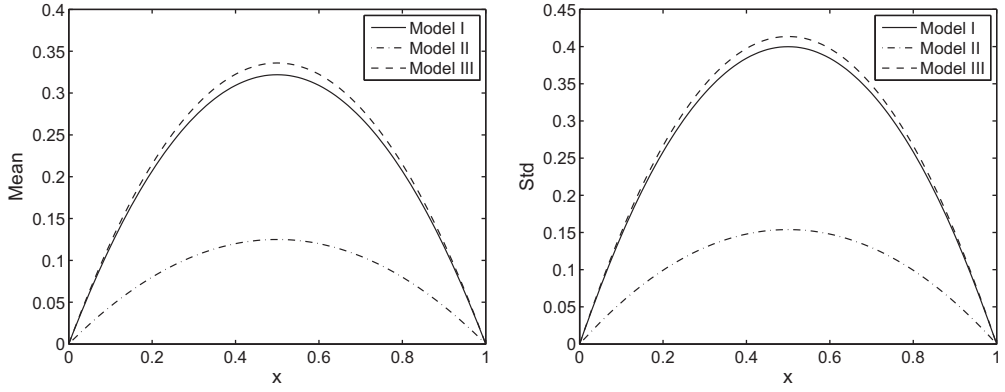

Fig. 1. Statistics of u_{I}, u_{II} and u_{III} when $\sigma = 1$ and $l = 5$. Left: mean and right: standard deviation.

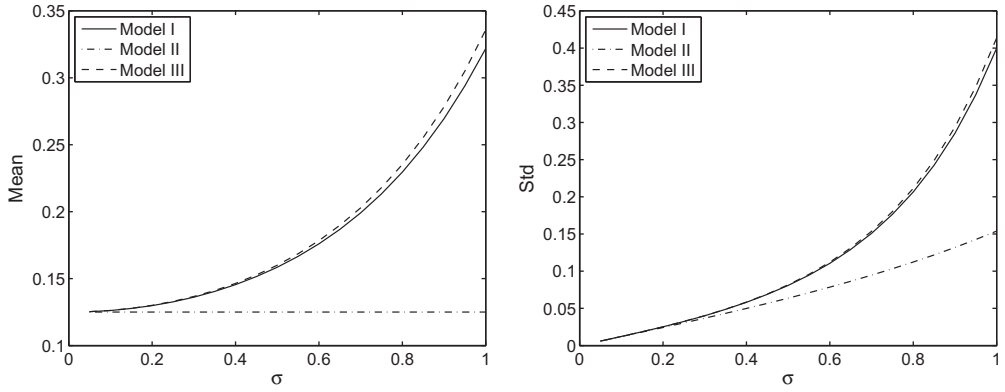

Fig. 2. Statistics of u_{I}, u_{II}, u_{III} at $x = 0.5$ with respect to σ.$l = 5$. Left: mean and right: standard deviation.

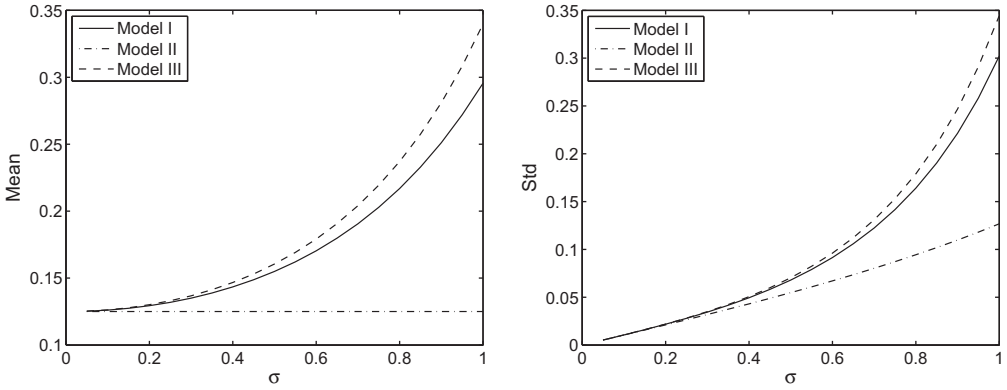

Fig. 3. Statistics of u_{I}, u_{II} and u_{III} at $x = 0.5$ with respect to σ. $l = 1$. Left: mean and right: standard deviation.

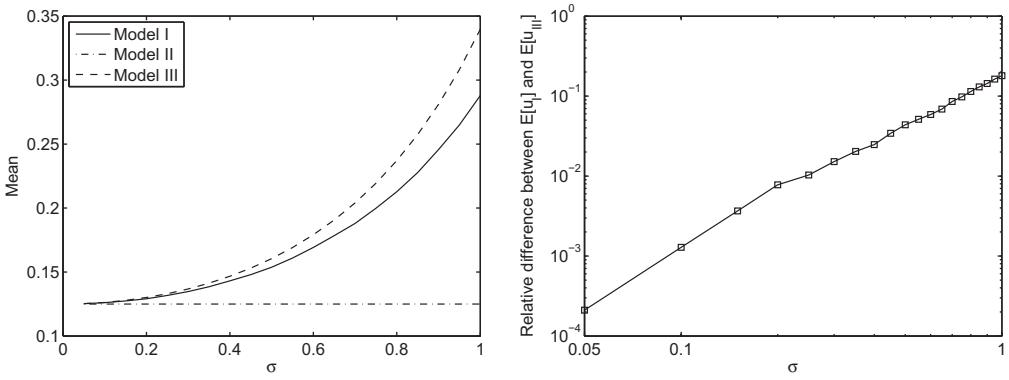

Fig. 4. $l = 0.1$. Left: mean of u_{I}, u_{II} and u_{III} at $x = 0.5$ with respect to σ and right: relative difference between $\mathbb{E}[u_{\mathrm{I}}]$ and $\mathbb{E}[u_{\mathrm{III}}]$.

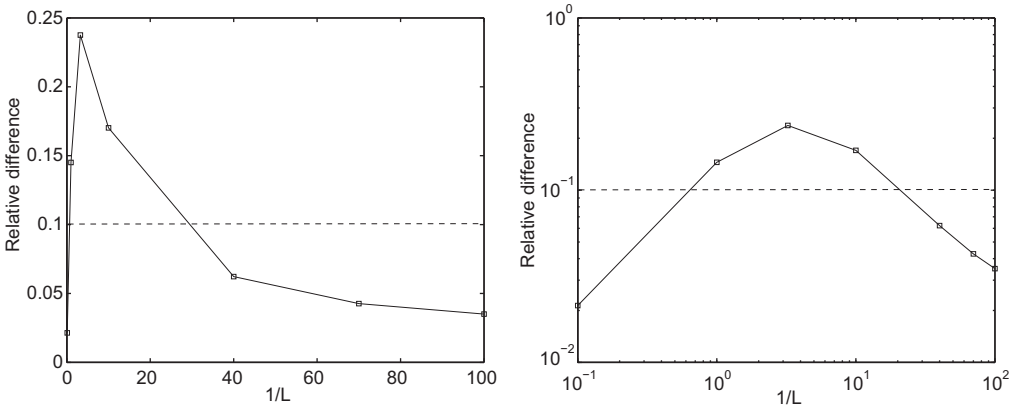

Fig. 5. Relative difference between $\mathbb{E}[u_{\mathrm{I}}]$ and $\mathbb{E}[u_{\mathrm{III}}]$ at $x = 0.5$ with respect to $1/l$ when $\sigma = 1$. Left: the original scale and right: the log–log scale.

the scaling factor e^{σ^2}, and $\mathbb{E}[u_{\mathrm{III}}]$ cannot see the variation of the correlation length l. From Figs. 2 and 3, it appears that the difference between $\mathbb{E}[u_{\mathrm{I}}]$ and $\mathbb{E}[u_{\mathrm{III}}]$ increases as the correlation length decreases for a certain σ.

We subsequently examine the difference between $\mathbb{E}[u_{\mathrm{I}}]$ and $\mathbb{E}[u_{\mathrm{III}}]$ for a much smaller correlation length compared to the physical domain. Since for a small correlation length l, a relatively large number of random variables is necessary to express the log-normal random process, we use the Monte Carlo method to deal with the high dimensionality. We consider correlation length $l = 0.1$ and 100 random variables for the K–L expansion of $W_\phi(x)$. The smallest eigenvalue is 0.11% of the largest one. In Fig. 4 we plot the mean solutions of u_{I}, u_{II} and u_{III} at $x = 0.5$ and the relative difference between $\mathbb{E}[u_{\mathrm{I}}]$ and $\mathbb{E}[u_{\mathrm{III}}]$ with respect to the degree of perturbation, where $\mathbb{E}[u_{\mathrm{I}}]$ is obtained by the Monte Carlo simulation with 100,000 realizations, $\mathbb{E}[u_{\mathrm{II}}]$ and $\mathbb{E}[u_{\mathrm{III}}]$ are computed exactly. When $\sigma = 1$, the relative difference between $\mathbb{E}[u_{\mathrm{III}}]$ and $\mathbb{E}[u_{\mathrm{I}}]$ is 17.98%. From the right plot in Fig. 4, we see that the relative difference increases overall algebraically. Roughly speaking, the relative difference is about $O(\sigma^2)$. It is also seen that when $\sigma \leqslant 0.7$, the difference is smaller than 10%. We note that $\sigma = 0.7$ corresponds to a degree about 80% of perturbation of $a(x,\omega)$.

One interesting question we have not answered yet is: Is there a limit of the relative difference between $\mathbb{E}[u_{\mathrm{I}}]$ and $\mathbb{E}[u_{\mathrm{III}}]$ for a certain

σ as the correlation length decreases? We have seen that when $\sigma = 1$, the relative difference between $\mathbb{E}[u_{\mathrm{I}}]$ and $\mathbb{E}[u_{\mathrm{III}}]$ is 4.34%, 14.98% and 17.98% corresponding to the correlation length 5, 1 and 0.1, respectively. In Fig. 5, we plot the evolution of the relative difference between $\mathbb{E}[u_{\mathrm{I}}]$ and $\mathbb{E}[u_{\mathrm{III}}]$ with respect to the inverse of correlation length, i.e., $1/l$, using different scales, i.e., a regular scale for the left plot and a log–log scale for the right plot. We use 1000 Gaussian random variables to represent the log-normal random process and 100,000 realizations for the Monte Carlo simulation. We can see from the left plot of Fig. 5 that the relative difference $\mathbb{E}[u_{\mathrm{I}}]$ and $\mathbb{E}[u_{\mathrm{III}}]$ first increases quickly as the correlation length decreases from infinity, and the relative difference reaches a limit about 24% when $l \approx 0.3$, then the relative difference will decrease gradually as the correlation length decreases. Furthermore, the increasing rate and the decreasing rate are roughly the same, see the right plot in Fig. 5. In Fig. 5, the dashed lines indicate a 10% relative difference. We see that the relative difference between $\mathbb{E}[u_{\mathrm{I}}]$ and $\mathbb{E}[u_{\mathrm{III}}]$ is less than 10% in an approximate region $l \in D_l := (0, \frac{1}{20}] \cup [2, \infty)$. In other words, $\mathbb{E}[u_{\mathrm{I}}]$ and $\mathbb{E}[u_{\mathrm{III}}]$ are comparable when the correlation length belongs to the region D_l when the degree of perturbation of $a(\boldsymbol{x}, \omega)$ is about 130%, i.e., $\sigma = 1$. By noticing that such a comparability is from the scaling factor e^{σ^2}, we know that when $l \in D_l$, the relative difference between $\mathbb{E}[u_{\mathrm{I}}]$ and $\mathbb{E}[u_{\mathrm{III}}]$ is dominated by the change of σ. We should note from previous studies that the region D_l will become larger when σ becomes smaller. In summary, although $\mathbb{E}[u_{\mathrm{III}}]$ cannot see the change in the correlation length of the underlying Gaussian process $W_\phi(x)$, it does provide a comparable mean solution with $\mathbb{E}[u_{\mathrm{I}}]$ for a large range of the correlation length l and the degree of perturbation σ.

5. Discussions

In this paper, we discussed two stochastic modeling strategies for elliptic problems, corresponding to models (I) and (II), respectively. Model (I) is widely used in engineering and physical applications while model (II) has a direct connection with Itô-Skorohod stochastic integration. We focused on the comparability of the statistics given by these two strategies. For a one-dimensional elliptic problem subject to a log-normal random coefficient, it was shown that the difference between models (I) and (II) is mainly from a scaling factor, which is an exponential function of the standard deviation of the underlying Gaussian random process. Based on such an observation, we proposed a new stochastic elliptic model, i.e., model (III), which is a variation of model (II). The main difference between models (II) and (III) is the way that we apply the Wick product. Specifically, models (I) and (III) shares the same aforementioned scaling factor, and numerical experiments for one-dimensional problems show that the first- and second-order moments of the solutions given by models (I) and (III) can be highly comparable.

Both $\mathbb{E}[u_{\mathrm{II}}]$ and $\mathbb{E}[u_{\mathrm{III}}]$ can be given by a deterministic PDE. For the log-normal coefficients chosen in this work, $\mathbb{E}[u_{\mathrm{I}}]$ is a function of both the degree of perturbation and the correlation length; $\mathbb{E}[u_{\mathrm{II}}]$ only depends on the mean of $a(\boldsymbol{x}, \omega)$ and cannot see the change of either the degree of perturbation or the correlation length; $\mathbb{E}[u_{\mathrm{III}}]$ is a function of the degree of perturbation. Numerical experiments for one-dimensional problems show that statistics of the solutions given by models (I) and (III) can be comparable for many cases, especially when the correlation length of the underlying Gaussian process is either small or large, or the standard deviation is small.

For the new stochastic elliptic model (III), there are some interesting open problems:

- Will u_{I} and u_{III} converge to the same solution as $l \to 0$ for one-dimensional problems? We note that for the one-dimensional case, the equation satisfied by $\mathbb{E}[u_{\mathrm{III}}]$ corresponds to the homogenized one-dimensional elliptic PDE.
- The aforementioned correspondence will not remain for two- and three-dimensional cases since the effective coefficients of the homogenized two- and three-dimensional elliptic PDEs do not take the form of a harmonic mean. For this case, it should be more interesting to quantify the difference between u_{I} and u_{III} with respect to σ. In the numerical experiments, we see that such a difference can be of $O(\sigma^2)$.
- From the numerical point of view, the comparability between models (I) and (III) is also an interesting issue. First, if the difference between u_{I} and u_{III} is small enough, it might be not necessary to use model (I) since the uncertainty propagator of model (III) can be approximated much more efficiently. Second, if it is necessary to approximate model (I), model (III) might provide an efficient preconditioner due to the small difference between u_{I} and u_{III} and the efficiency to obtain u_{III}.

Studies on these topics are in progress and the above questions are partially answered in [19].

Acknowledgements

This work is supported by DOE Grant SC0002324 and the Louisiana State University Council on Research Summer Stipend Program of 2010.

References

[1] I. Babuška, R. Tempone, G. Zouraris, Galerkin finite element approximations of stochastic elliptic differential equations, SIAM J. Numer. Anal. 42 (2004) 800–825.
[2] I. Babuška, F. Nobile, R. Tempone, A stochastic collocation method for elliptic partial differential equations with random input data, SIAM J. Numer. Anal. 45 (2007) 1005–1034.
[3] R. Cameron, W. Martin, The orthogonal development of nonlinear functionals in series of Fourier–Hermite functionals, Ann. Math. 48 (1947) 385.
[4] R. Ghanem, P. Spanos, Stochastic Finite Element: A Spectral Approach, Springer-Verlag, New York, 1991.
[5] P. Frauenfelder, C. Schwab, R. Todor, Finite elements for elliptic problems with stochastic coefficients, Comput. Methods Appl. Mech. Engrg. 194 (2005) 205–228.
[6] R. Todor, C. Schwab, Convergence rates for sparse chaos approximations of elliptic problems with stochastic coefficients, IMA J. Numer. Anal. 27 (2) (2007) 232–261.
[7] H. Holden, B. Oksendal, T. Zhang, Stochastic Partial Differential Equations: A Modeling, White Noise Functional Approach, Birkhauser, Boston, 1996.
[8] M. Jardak, C.-H. Su, G. Karniadakis, Spectral polynomial chaos solutions of the stochastic advection equation, J. Sci. Comput. 17 (2002) 319–338.
[9] S. Lototsky, B. Rozovskii, Stochastic differential equations driven by purely spatial noise, SIAM J. Math. Anal. 41 (4) (2009) 1295–1322.
[10] S. Lototsky, B. Rozovskii, X. Wan, Elliptic equations of higher stochastic order, ESAIM: Math. Modell. Numer. Anal. 5 (4) (2010) 1135–1153.
[11] D. Nualart, Malliavin Calculus and Related Topics, second ed., Springer, New York, 2006.
[12] D. Nualart, B. Rozovskii, Weighted stochastic Sobolev spaces and bilinear SPDE's driven by space-time white noise, J. Funct. Anal. 149 (1997) 200–225.
[13] J. Galvis, M. Sarkis, Aproximating infinity-dimensional stochastic Darcy's equations without uniform ellipticity, SIAM J. Numer. Anal. 47 (5) (2010) 3624–3651.
[14] G. Papanicolaou, Diffusion in random media, in: J.B. Keller, D. McLaughlin, G. Papanicolaou (Eds.), Surveys in Applied Mathematics, Plenum Press, New York, 1995, pp. 205–255.
[15] F. Riesz, B. Sz-Nagy, Functional Analysis, Dover, New York, 1990.
[16] T. Theting, Solving Wick-stochastic boundary value problems using a finite element method, Stochastics Stochastics Rep. 70 (2000) 241–270.
[17] G. Våge, Variational methods for PDEs applied to stochastic partial differential equations, Math. Scand. 82 (1998) 113–137.
[18] X. Wan, B. Rozovskii, G. Karniadakis, A stochastic modeling methodology based on weighted Wiener chaos and Malliavin calculus, Proc. Natl. Acad. Sci. USA 106 (2009) 14189–14194.
[19] X. Wan, A discussion on two stochastic elliptic modeling strategies, Commun. Comput. Phys., submitted for publication.